

Observation of Cold Scission of Highly Excited Fissioning Nuclei

D. Hilscher, H. Rossner, B. Cramer, B. Gebauer, U. Jahnke, M. Lehmann, E. Schwinn, M. Wilpert, and Th. Wilpert

Hahn-Meitner-Institut Berlin, 1000 Berlin 39, Federal Republic of Germany

H. Frobeen, E. Mordhorst, and W. Scobel

Universität Hamburg, 2000 Hamburg 50, Federal Republic of Germany

(Received 28 November 1988)

The time scale of fission at initial nuclear temperatures of about 5 MeV is deduced from the number of neutrons evaporated prior to and after scission in the reactions ^{144}Sm and $^{154}\text{Sm} + (838 \text{ MeV}) \text{ }^{32}\text{S}$. The prescission lifetime for fission with symmetric mass splits is longer than for asymmetric mass splits. For symmetric mass splits the excitation energy at scission is only about 60 MeV and independent of the initial excitation energy which is consistent with a prescission lifetime in the order of 10^{-20} s.

PACS numbers: 25.70.Jj, 25.70.Gh, 25.85.Ge, 27.70.+q

Fifty years after the discovery of nuclear fission the dynamics of the division of the nucleus into two parts of roughly equal size is still one of the most interesting processes of collective flow of nuclear matter and an ideal example of the yet unsolved nuclear many-body problem. The time scale of nuclear fission has recently been studied¹⁻⁴ very intensively up to nuclear temperatures of about 2.7 MeV by several groups. One method employed¹⁻³ the number of neutrons evaporated prior to scission to deduce the prescission lifetime by calculating the mean evaporation time and thus relating the prescission neutron multiplicity with an absolute time scale. A second method⁴ exploited the giant-dipole-resonance γ rays emitted from the composite systems produced in heavy-ion-fusion reactions. Both methods led to the conclusion that nuclear fission at temperatures up to 2.7 MeV is very slow, about a few 10^{-20} s. In other words, nuclear fission, or rather scission, occurs at the very end of the nuclear deexcitation chain. An exciting question, then, is whether this finding prevails also at higher excitation energies or nuclear temperatures. In the present experiment we have investigated for the first time the fission time scale of nuclei at initial temperatures of about 5 MeV or excitation energies of about 500–600 MeV in nuclei of mass close to 180. Furthermore, we have measured for the first time the time scale of fission with symmetric and asymmetric mass splits. At such high temperatures one might expect that the temperature dependence of the nuclear surface tension⁵ and/or nuclear dissipation⁶ could drastically influence the time scale of nuclear fission. In the following we will briefly discuss the experiment and then present the results for the number of neutrons emitted prior to and after scission, which we use to establish a relative and, with certain assumptions, absolute time scale.

Targets of isotopically enriched ^{144}Sm and ^{154}Sm with thicknesses of 185 and 216 $\mu\text{g}/\text{cm}^2$, respectively, on carbon backings of 50 $\mu\text{g}/\text{cm}^2$ were bombarded with 838-

MeV ^{32}S ions at the VICKSI accelerator in Berlin. Two heavy fragments were detected in coincidence with two x and y position-sensitive low-pressure multiwire chambers providing also good time resolution of about 0.2 ns. The absolute time-of-flight resolution in reference to the cyclotron frequency was 0.8 ns. The centers of these detectors were positioned to the left and right of the beam at $\Theta_1 = -43.6^\circ$, $\Theta_2 = 54.5^\circ$ defining the reaction plane and subtending in- and out-of-plane angular ranges of $\Delta\Theta_1 = \pm 6^\circ$, $\Delta\Phi_1 = \pm 6^\circ$ and $\Delta\Theta_2 = \pm 22^\circ$, $\Delta\Phi_2 = \pm 12^\circ$, respectively. In addition to the four angles Θ_1 , Φ_1 , Θ_2 , and Φ_2 the time of flight of the fragments was measured. The path lengths for the central rays were $L_1 = 24.3$ cm and $L_2 = 27.8$ cm. With those measured quantities the velocity vectors of both fragments and the mean velocity v_0 of the composite system are known. From the ratio of the transverse velocity components the mean mass ratio at scission can be determined. This ratio is converted into absolute mass numbers by normalization to the initial composite mass. The thus determined mass A_2 of one fragment is shown in Fig. 1 versus the folding angle $\Theta_1 + \Theta_2$ in a contour diagram. The contour lines are shown for 10% to 90% in steps of 10% of the maximum yield. The dotted lines show the expectation for $A_2 \times (\Theta_1 + \Theta_2)$ assuming linear-momentum transfer (LMT) of 100% (left) to 50% in steps of 10% of complete fusion and employing the massive transfer model and total kinetic energies as given by the Viola systematics.⁷ The ratio of moments of inertia $J_{\text{orbital}}/J_{\text{rigid-body}}$ was used to calculate the fraction of the rotational energy of the compound nucleus with an assumed spin of $80\hbar$ contributing to the total kinetic energy (≈ 6 MeV). Figure 1 shows that the maximum yield of symmetric mass splits corresponds to about 80% LMT. Furthermore, it is interesting to note that the dotted line never reaches the ridge of maximum yield for the heavier fragment masses. This is already an indication that mass loss occurs prior to scission, in addition to the one taken into account in

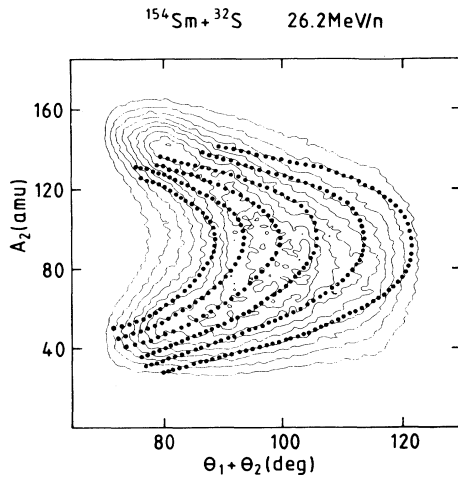


FIG. 1. Contour diagram of coincident fragment yield as a function of the folding angle and the mass of fragment A_2 . The total kinetic energies were between about 90 and 180 MeV with a mean value of about 135 MeV.

the massive transfer model. To some lesser extent this can also be attributed to higher angular momenta associated with asymmetric mass splits.

For all results shown in this investigation the requirement for the total kinetic energies for the fragments was 100 to 200 MeV with a mean value of about 150 MeV without correction for prescission particle emission. If corrections are performed for mass loss prior to scission of about 8% to 10% of $A_{\text{projectile}} + A_{\text{target}}$, these values have to be decreased correspondingly, in which case the fragment kinetic energies are within the experimental uncertainties of about 5 to 10 MeV equal to the Viola values.⁷ Thus the available kinetic energy which was not removed promptly by preequilibrium light particles has been dissipated into internal degrees of freedom.

Neutron energy spectra were measured at nine angles in and out of plane in coincidence with the two fission fragments. The prescission and postsission neutron multiplicities were determined by exploiting the kinematical focusing of the neutrons into the spatial direction into which the emitting source is moving. The measured energy spectra were fitted with analytic expressions resulting from the assumption of four moving sources emitting neutrons isotropically in the respective rest frames with spectra distributions $M_n \sqrt{E_n} e^{-E_n/T_n}$, where M_n , E_n , and T_n are the neutron multiplicity, emission energy, and the mean temperature, respectively. The four assumed sources are (1) the composite system moving with a velocity v_0 (as measured), (2) and (3) the fragments moving with the measured velocities v_1 and v_2 , and (4) a preequilibrium component moving with an assumed velocity of half the beam velocity in accordance with systematic investigations of preequilibrium nucleon emission in central collisions.⁸ The parameters searched for

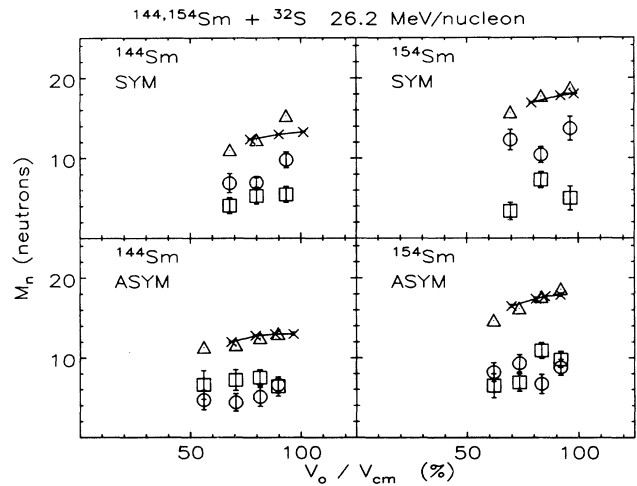


FIG. 2. Multiplicity of neutrons emitted prior to (circles) and after (squares) scission and the sum of both (triangles) for symmetric (SYM: $\langle A_1 \rangle = \langle A_2 \rangle = 76-120$) and asymmetric (ASYM: $A_1 = 20-75$ and $A_2 = 121-160$) mass splits. The crosses connected with a solid line are the result of the measurement of the total neutron multiplicity with the neutron sphere.

in the least-squares fit of all nine measured neutron energy spectra were the four neutron multiplicities and temperatures for each source. Further details of the fitting procedures and the validity of the assumptions made in the search routine are described by Zank *et al.*³

The results of those fits are shown in Fig. 2 for the neutron multiplicity from the composite system (source 1, circles) and from both fragments (sum of sources 2 and 3, squares) which we identify with the numbers of neutrons evaporated prior to and after scission, respectively. The multiplicities are plotted versus the ratio of v_0 and the center-of-mass velocity $v_{c.m.}$, which is a measure of the actual linear-momentum transfer. The multiplicity for symmetric and asymmetric mass splits are shown in the top and lower parts of Fig. 2, respectively. The triangles are the sum of prescission and postsission neutrons which have to be compared with the crosses. The crosses are the result of an independent measurement of the total neutron multiplicity of the same reaction with the neutron ball^{9,10} which measures each emitted neutron with a high efficiency of 87%. The setup for the fragment measurement in the latter experiment was as similar to the above-described experiment as possible. Two multiwire chambers of the smaller type (defining Θ_1, Φ_1 in the above-described setup) were used at distances reduced by about a factor of 2 in order to fit them into the smaller scattering chamber inside the neutron sphere. Furthermore, the samarium targets were about a factor of 4 thicker ($750 \mu\text{g}/\text{cm}^2$ metallic samarium). The agreement is excellent with the time-of-flight data.

Figure 2 demonstrates very clearly that for symmetric

mass splits the precission neutrons multiplicity is considerably larger than the number of postscission neutrons whereas for asymmetric mass splits the number of neutrons emitted prior to and after scission are about equal. The total neutron multiplicities are the same for symmetric mass splits. This first finding demonstrates already without any further assumptions that fission with symmetric mass splits is slower than fission processes with asymmetric mass splits. Symmetric mass splits can be associated with fission from a system equilibrated in energy and mass degree of freedom resulting probably from more central collisions than asymmetric mass splits which carry more angular momentum.

The second finding which we can read off immediately from Fig. 2 is the small number of postscission neutrons of 5.5 ± 1.3 and 5.0 ± 1.5 neutrons for both fragments in the reactions on ^{144}Sm and ^{154}Sm and the maximum linear-momentum transfer bins with mean values of $v_0/v_{c.m.} = 0.93$ and 0.96 , respectively. This observation means that most of the excitation energy has been essentially removed until the system has reached the scission point. Employing this number of postscission neutrons we can calculate the excitation energy at scission to be about 60 MeV. This result is essentially independent of the amount of initial excitation energy, as can be seen from Fig. 3 where the number of postscission neutrons measured previously for a composite system with $Z_{CN} = Z_{\text{projectile}} + Z_{\text{target}} = 77$ are compared with the present

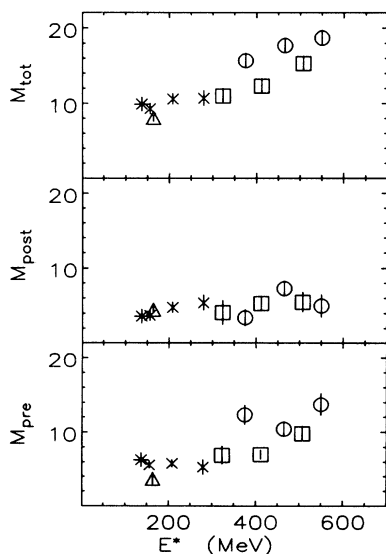


FIG. 3. Precission M_{pre} , postscission neutron multiplicity (sum of neutrons emitted from both fragments) M_{post} , and total number of evaporated neutrons $M_{\text{tot}} = M_{\text{pre}} + M_{\text{post}}$ as a function of the initial excitation energy for $Z_{CN} = 77-78$. Squares and circles are the present result for different LMT in fission induced by ^{32}S on ^{144}Sm and ^{154}Sm , respectively. Crosses are the result of the reaction $^{165}\text{Ho} + ^{20}\text{Ne}$ (Ref. 11), triangles for $^{141}\text{Pr} + ^{40}\text{Ar}$, and stars for $^{175}\text{Lu} + ^{12}\text{C}$ (Ref. 3).

result for $Z_{CN} = 78$. The number of postscission neutrons at excitation energies above about 140 MeV levels off at about 5 neutrons whereas the precission and total neutron multiplicities are increasing with increasing excitation energy.

If we assume that we know the absolute level densities, we can go one step further and calculate the mean neutron-decay width $\Gamma_n(E^*)$ and thus also the mean evaporation time $\tau_n = \hbar/\Gamma_n$. By summing over the neutrons evaporated from the composite system we can plot the average lifetime as a function of the number of neutrons evaporated from the composite system. This is done in Fig. 4, where the calculated mean neutron evaporation time of compound nuclei $^{176}\text{Pt} = ^{144}\text{Sm} + ^{32}\text{S}$ and $^{186}\text{Pt} = ^{154}\text{Sm} + ^{32}\text{S}$ with initial excitation energies of 507 and 550 MeV is plotted versus the precission neutron multiplicity. The level-density parameter was assumed¹² to be $a = A/10$ MeV⁻¹ and the decay by n , p , d , α , and γ emission has been considered. By exploiting the experimental values for the precission multiplicity for symmetric mass splits of 9.8 ± 1.0 and 13.7 ± 1.5 for ^{144}Sm and ^{154}Sm at linear-momentum transfers of $v_0/v_{c.m.} = 0.93$ and 0.96 , respectively, we can read off for both targets a precission lifetime of $\tau_s \approx 8 \times 10^{-21}$ s whereas for asymmetric mass splits we obtain only $\tau_a \approx 3 \times 10^{-21}$ s, employing the corresponding precission neutron multiplicities of 6.6 ± 1.0 (^{144}Sm) and 8.8 ± 1.0 (^{154}Sm). The uncertainties of the absolute time values τ are hard to estimate. However, the underlying high precission neutron multiplicities seem to be incompati-

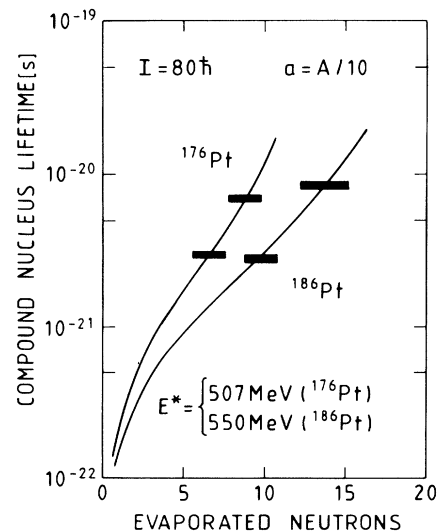


FIG. 4. Calculated evaporation time (solid lines) of N neutrons from the compound nuclei $^{176}\text{Pt} = ^{144}\text{Sm} + ^{32}\text{S}$ and $^{186}\text{Pt} = ^{154}\text{Sm} + ^{32}\text{S}$ at initial excitation energies of 507 and 550 MeV, respectively, and at a mean angular momentum of $80\hbar$. The measured precission neutron multiplicities at the maximum LMT bin are indicated by bars for symmetric and asymmetric mass splits.

ble with considerably shorter scission times, e.g., 6×10^{-22} s of the random-neck-rupture model.¹³ Also, the ratio $\tau_s/\tau_a \approx 2$ is in first-order independent of the level densities applied: Asymmetric fission turns out to be the faster process.

It is interesting to note that the calculated pre-scission time as shown in Fig. 4 is essentially determined by the last few evaporated pre-scission neutrons whereas the evaporation times of the first evaporated neutrons are too small to strongly influence the pre-scission lifetime. This observation has three important consequences: (i) The level densities at excitation energies around 100 MeV essentially determine the extracted pre-scission lifetime and not at excitation energies around 500 MeV where they are considerably less certain, (ii) the collective motion of nuclear matter within the first $\sim 10^{-22}$ s during which the dinuclear temperature is at ~ 5 MeV will be small and thus the investigation of a temperature dependence of the nuclear viscosity or the nuclear dissipation as for instance calculated theoretically by Yamaji *et al.*⁶ will be difficult if not impossible with the present method, and (iii) the excitation energy at scission and thus also the post-scission neutron multiplicity measures essentially the pre-scission lifetime. Neglecting the change in fission Q values due to pre-scission particle emission, this latter observation would result in an approximately constant, that is independent of the initial excitation energy, post-scission neutron multiplicity for a constant pre-scission lifetime. This is exactly what can be observed in Fig. 3: $M_{\text{post}} \approx 5$ neutrons.

In summary, we conclude that fission with symmetric

mass splits from a composite system at nuclear temperatures of about 5 MeV or excitation energies of 500 to 600 MeV is still a slow process occurring at the very end of the nuclear deexcitation chain and leaving the fissioning system at relatively low excitation energy at scission of about 60 MeV. The observation of a low excitation energy at scission is essentially independent of the initial excitation energy. The fragments are probably strongly deformed at scission so that the thermal excitation energy at the scission configuration might be even smaller. With certain assumptions for the absolute level densities and neglecting such deformations we have shown that the pre-scission lifetime is in the order of 10^{-20} s even at the high excitation energies reached in the present investigation. Finally we have observed that the pre-scission lifetime for fission into asymmetric mass splits is shorter than for symmetric mass splits.

-
- ¹D. J. Hinde *et al.*, Nucl. Phys. **A452**, 550 (1986).
 - ²A. Gavron *et al.*, Phys. Rev. C **35**, 579 (1987).
 - ³W. P. Zank *et al.*, Phys. Rev. C **33**, 519 (1986).
 - ⁴M. Thoennessen *et al.*, Phys. Rev. Lett. **59**, 2860 (1987).
 - ⁵R. W. Hasse and W. Stocker, Phys. Lett. **44B**, 26 (1973).
 - ⁶S. Yamaji *et al.*, Nucl. Phys. **A475**, 487 (1988).
 - ⁷V. E. Viola *et al.*, Phys. Rev. C **31**, 1550 (1985).
 - ⁸D. Hilscher, Nucl. Phys. **A471**, 77 (1987).
 - ⁹U. Jahnke *et al.*, Phys. Rev. Lett. **50**, 1246 (1983).
 - ¹⁰K. Hagel *et al.*, Nucl. Phys. **A486**, 429 (1988).
 - ¹¹D. Hilscher *et al.*, Phys. Rev. C **36**, 208 (1987).
 - ¹²U. Brosa and S. Grossmann, Z. Phys. A **310**, 177 (1983).
 - ¹³E. Holub *et al.*, Phys. Rev. C **28**, 252 (1983).